Simultaneous Photoproduction of η and π^0 Mesons on the Proton

J. Ajaka,[1] Y. Assafiri,[1] O. Bartalini,[2] V. Bellini,[3] S. Bouchigny,[1] M. Castoldi,[4] A. D'Angelo,[2] J. P. Didelez,[1] R. Di Salvo,[2] M. Döring,[5] A. Fantini,[2] L. Fichen,[1] G. Gervino,[6] F. Ghio,[7] B. Girolami,[7] A. Giusa,[3] M. Guidal,[1] E. Hourany,[1,*] R. Kunne,[1] A. Lapik,[8] P. Levi Sandri,[9] D. Moricciani,[2] A. Mushkarenkov,[8] V. Nedorezov,[8] E. Oset,[10] C. Randieri,[3] N. Rudnev,[8] G. Russo,[3] C. Schaerf,[2] M. Sperduto,[3] M. Sutera,[3] and A. Turinge[11]

[1]*IN2P3, Institut de Physique Nucléaire, 91406 Orsay, France*
[2]*INFN, sezione di Roma II and Università di Roma "Tor Vergata," 00133 Roma, Italy*
[3]*INFN, Laboratori Nazionali del Sud and Università di Catania, 95123 Catania, Italy*
[4]*INFN, sezione di Genova, 16146 Genova, Italy*
[5]*University of Georgia, Athens GA 30602, USA*
[6]*INFN, sezione di Torino and Università di Torino, 10125 Torino, Italy*
[7]*INFN, sezione Sanità and Istituto Superiore di Sanità, 00191 Roma, Italy*
[8]*Institute for Nuclear Research, 117 312 Moscow, Russia*
[9]*INFN, Laboratori Nazionali di Frascati, 00044 Frascati, Italy*
[10]*Departamento de Física Teórica and IFIC, Centro Mixto Universidad de Valencia-CSIC, 46071 Valencia, Spain*
[11]*I. Kurchatov Institute of Atomic Energy, Moscow, Russia*
(Received 5 September 2007; published 8 February 2008)

The analysis of the $\gamma p \to \eta\pi^0 p$ reaction has been performed using data from the GRAAL experiment. The total and differential cross sections and the beam asymmetry have been obtained from threshold up to 1.5 GeV of beam energy. The two resonances $S_{11}(1535)$ and $\Delta(1700)$ are expected to be excited in the intermediate states of this reaction. The results are used to test predictions based on the assumption that both resonances are dynamically generated from the meson-baryon interaction provided by chiral Lagrangians. The term involving the $\Delta(1700)$ excitation, followed by the decay into $\eta\Delta(1232)$, is found to be dominant.

DOI: 10.1103/PhysRevLett.100.052003 PACS numbers: 13.60.Le, 13.88.+e, 14.40.Aq

Recently, double π^0 photoproduction on the nucleon, with protons and neurons, was studied at GRAAL and used as a tool for baryonic resonance spectroscopy [1,2]. Here we consider the GRAAL data to study the more exotic reaction, $\gamma p \to \eta\pi^0 p$. It happens that this new reaction is now of great interest for the study of two resonances generated dynamically in a chiral unitary approach and consisting of quasibound states of a meson and a baryon, the $S_{11}(1535)$ and the $\Delta(1700)$. The chiral unitary approach combines the information contained in the chiral Lagrangians (see [3,4] for the case of the meson-baryon interaction), which provides an effective representation of QCD at low energies, with the constraints of unitarity in coupled channels [5–7]. The nonperturbative treatment of the problem, using the Bethe Salpeter equation or equivalent formalisms, sometimes generates poles in the scattering matrix which correspond to resonances that we call "dynamically generated." Recent theoretical results along these lines [5,8] found that the $S_{11}(1535)$ is one of the states dynamically generated which appears from the interaction of the octet of pseudoscalar mesons with the octet of baryons of the nucleon. Also the $\Delta(1700)$ is generated dynamically from the interaction of the octet of pseudoscalar mesons with the decuplet of baryons of the Δ [9,10]. The model of Refs. [11,12] built on a chiral unitary theory predicts the observables of the $\gamma p \to \eta\pi^0 p$ reaction where the resonances $\Delta(1700)$ and $S_{11}(1535)$ are intermediate states and have the properties of dynamically generated resonances. The other existing model [13] was not applied to predict the observables of the present reaction. In the present Letter, we describe the method of analysis for the $\gamma p \to \eta\pi^0 p$ reaction and present the total cross section, the invariant mass spectra of each pair of particles in the final state and the beam asymmetry observables. The experimental results will be compared with the results of the theoretical model [11,12] which are reported here for the first time.

The data have been obtained with the GRAAL setup using a tagged and linearly polarized photon beam, a 12 cm thick liquid hydrogen target, and a 4π detector [14]. The photon beam is produced by backscattering laser light on the 6.04 GeV electron beam in the European Synchrotron Radiation Facility (ESRF) ring at Grenoble. The energy spectrum of the photon beam is flat and the degree of polarization is close to 100% at the maximum energy. Choosing the UV line of the laser, the energy of the produced photon beam used here varies between the threshold (932 MeV) and the maximum of 1500 MeV with a degree of polarization ranging from 0.6 to 0.96. The beam intensity was close to $1.0 \times 10^6 \gamma/\mathrm{s}$.

The large acceptance detector consists of three layers: wire chambers, scintillators, and calorimeters. In the central part ($25° \leq \theta \leq 155°$), a bismuth germanate (BGO) calorimeter (90% of 4π, energy resolution 3% for γ's),

 © 2008 The American Physical Society

centered on the target and vetoed by a barrel of scintillators measures with a good resolution the energy and angles of the γ's. In the forward direction ($\theta \leq 25°$), a double wall of scintillators and a shower wall measure the time of flight of the proton and the neutron, respectively.

In the analysis, the experimental events having one charged and four neutral particles (expected to be 4γ's) detected in the final state are selected. Among these events, a further selection retains only those events with the 4 neutral particles falling in the BGO detector acceptance to ensure a good energy measurement of the expected γ's. The identification of the charged particle as being a proton is done: (i) with the time of flight given by the scintillator wall when the proton is emitted in the forward direction, and (ii) with the energy loss in the scintillator barrel when it is detected by the central detector. The angles of the 4γ's and of the charged particle are determined using the cellular structure of the detector and the vertex of the reaction assuming, to begin with, that the vertex of the reaction is the center of the target.

The four neutral particles are used to search for two mesons η and π^0, each one decaying into 2γ's. For this purpose, the 4γ's are grouped into two pairs and for each pair the invariant mass is calculated. Six configurations of the possible pairs are considered before selecting the ''best configuration'' in which the invariant mass of one pair is closest to the mass of the π^0 while that of the other pair is close to the η mass. The conservation of momentum and energy is used to calculate the kinematical variables of the reaction and, in addition, to determine the vertex position on the axis of the target. During this procedure it became clear that the abundance of events coming from the reaction $\gamma p \to \pi^0\pi^0 p$ which were processed as being due to the reaction $\gamma p \to \eta\pi^0 p$, produced a high background. In order to recognize these events and reject them, the analysis included a part that assumes each event as belonging to $\gamma p \to \pi^0\pi^0 p$. Combining the 4γ's into three combinations of invariant masses (IM) M_1 and M_2, the quadratic deviation with respect to $2\pi^0$'s masses $[D_{\pi^0\pi^0}{}^2 = (M_1 - M_{\pi^0})^2 + (M_2 - M_{\pi^0})^2]$ was calculated and the combination giving the minimum deviation was stored.

Figures 1(a) and 1(b) show the spectra of η and π^0 masses for the events analyzed as $\gamma p \to \eta\pi^0 p$ events, while (c) shows the quantity $D_{\pi^0\pi^0}$ when the same events are analyzed as $\gamma p \to \pi^0\pi^0 p$ events. Thick lines correspond to spectra without cuts: the panels (a) and (b) show well-resolved η and π^0 peaks on a high background, and in (c) the curve is strongly peaked around the value zero, which is the location of $2\pi^0$'s. With a line of normal thickness, panels (a) and (b) are drawn after a cut on the events having $D_{\pi^0\pi^0} \leq 0.02$ GeV, and (c) shows the spectrum obtained after the simultaneous selection, labeled $S_{\pi^0\eta}$, through the two windows of $0.4750 \leq M(\eta) \leq 0.625$ GeV and of $0.105 \leq M(\pi^0) \leq 0.165$ GeV. The thinnest lines on panels (a) and (b) are obtained with the

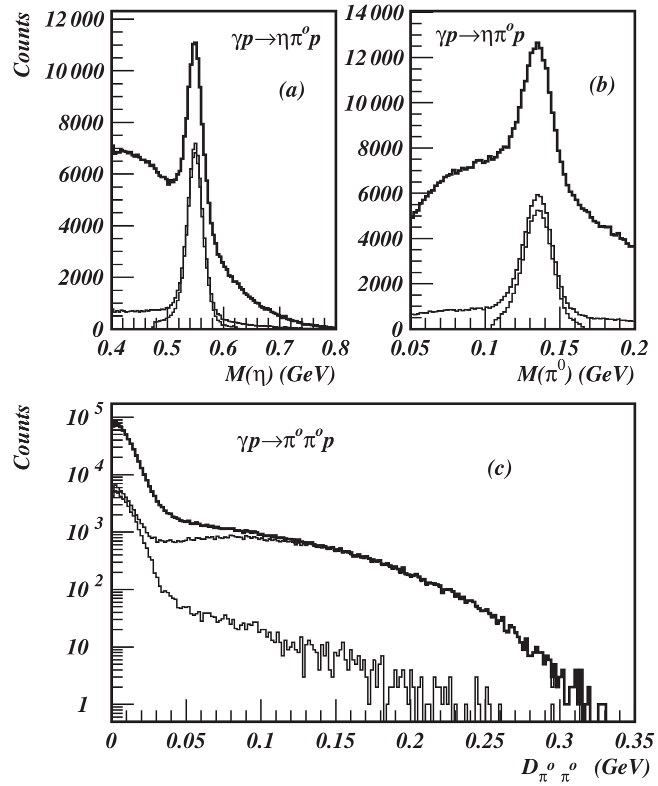

FIG. 1. Extraction of the $\gamma p \to \eta\pi^0 p$ events. Panels (a) and (b) show the constructed spectra of η and π^0, respectively, with the assumption that the event belongs to the $\gamma p \to \eta\pi^0 p$ reaction (resolution of 22 MeV for the π^0 and of 30 MeV for the η) and panel (c), the quadratic deviation of the masses of $2\pi^0$'s from the constructed masses with the assumption that the event belongs to the $\gamma p \to \pi^0\pi^0 p$ reaction. With thick, normal, and thin lines, the same results but after the selections explained in the text.

combined $D_{\pi^0\pi^0} \leq 0.02$ GeV condition and the selection $S_{\pi^0\eta}$. Clean peaks are observed. However there is still a residual contamination due to a background from $\gamma p \to \pi^0\pi^0 p$ events where the $M(\eta)$ component is under the $M(\eta)$ peak simultaneously with the $M(\pi^0)$ component under the $M(\pi^0)$ peak. This contamination was estimated (in order to be subtracted) from the events having their $M(\eta)$ component under the $M(\eta)$ peak and their $M(\pi^0)$ component at the wings of the $M(\pi^0)$ peak. With a thin line, panel (c) shows the spectrum of the estimated contamination.

A total number of 61 000 pure $\gamma p \to \eta\pi^0 p$ events were extracted. The total residual background amounts to 6%. As to the events of the reaction $\gamma p \to \eta\pi^0 p$, cut with the condition $D_{\pi^0\pi^0} \leq 0.02$ GeV, they were estimated to constitute only 2% of the total events.

In parallel to the analysis of the experimental data, a simulation calculation was carried out using the code LAGGEN of GRAAL built on an event generator and on the GEANT3 code from the CERN library, which provides the tracking of the produced particles in the detector. The results of the simulation were used for the efficiency determination and the obtention of IM spectra. For the acceptance calculation of the reaction $\gamma p \rightarrow \eta\pi^0 p$, let us notice that the proton is detected at all angles and energies with an efficiency of $\approx 100\%$ and that the π^0 and η mesons are detected with an efficiency of $\approx 100\%$ except when one or more among the 4γ are emitted with a $\theta_\gamma \leq 25°$. One can deduce that instead of depending on the 5 independent variables of the final state the acceptance depends only on the variables θ_η and θ_{π^0}, with a hole (efficiency null) for $\theta_{\pi^0} \leq 12°$. In the event generator we used the phase spaces of various types available in the code LAGGEN: (1) $\gamma p \rightarrow \eta\pi^0 p$, with a 3-body phase space, (2) $\gamma p \rightarrow \eta\Delta$ with $\Delta \rightarrow \pi^0 p$, and (3) $\gamma p \rightarrow \pi^0 S_{11}$ with $S_{11} \rightarrow \eta p$. For each type, large numbers of generated events were processed with the same programs as used for the data. The events before and after the processing were binned into a tridimensional space E_γ, θ_{π^0}, and θ_η, with 15 bins in E_γ ranging from 0.95 to 1.5 GeV, 14 bins in θ_{π^0} from 0° to 168° and 12 bins in θ_η from 0° to 84°. The comparison of the cell contents before and after processing gave the efficiency $\epsilon(E_\gamma, \theta_{\pi^0}, \theta_\eta)$ and the amount of extrapolation at each energy to recover for the hole in the θ_{π^0} variable.

To calculate the total cross section, the events were again binned in the tridimensional space E_γ, θ_{π^0}, and θ_η. The content of each cell of the tridimensional space was cleaned for background and corrected for the efficiency. After the normalization by the beam flux and taking into account the branching ratio of η into 2γ's equal to 0.3938 [15], the total cross section was plotted with solid circles against the beam energy in Fig. 2. The cross section increases up to a value of 3.5 μb at $E_\gamma = 1.5$ GeV. Systematic errors due to the beam flux determination, the acceptance calculation, and the background subtraction are estimated to be $\approx 7\%$ and are included in the errors plotted in the figure. These results are compatible with those of Ref. [16] measured at low energies ($E_\gamma \leq 1.15$ GeV) and plotted with open circles.

The results of the model described above for the total cross section are plotted with a hatched band in Fig. 2. The uncertainty band comes from the uncertainty on the $\gamma p\Delta(1700)$ coupling which was taken from the PDG [15]. Here the shape and magnitude of the total cross section are reproduced, which confirms the effect of the large coupling of the dynamically generated resonance $\Delta(1700)$ to $K\Sigma(1385)$ and $\eta\Delta$. The square of the ratios of the couplings of these channels to the $\Delta\pi$ are 20–30 times larger than the one obtained in the frame of pure SU(3) symmetry assuming the $\Delta(1700)$ is a member of a decuplet as suggested in the PDG [15] (p. 169). The numbers for the couplings of the dynamically generated $\Delta(1700)$ resonance are shown in Table 10 of [10]. In particular $|g_{\Delta^*\eta\Delta}| = 2.2$, is comparatively large. The

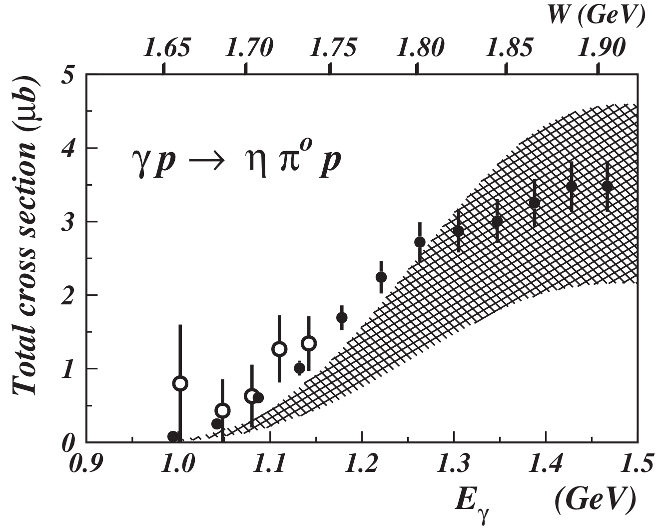

FIG. 2. Total cross section of the reaction $\gamma p \rightarrow \eta\pi^0 p$. The dots are the experimental data of this work. The open circles are from Ref. [16]. The results of the model of Refs. [11,12] are given with their uncertainty by a hatched band of the figure. The uncertainty originates from the one on the $\gamma p\Delta(1700)$ coupling which was taken from the PDG [15].

$\Delta(1700) \rightarrow \eta\Delta(1232)$ decay width obtained with this coupling by folding the width with the mass distribution of the $\Delta(1700)$ and $\Delta(1232)$ leads to a branching ratio of the order of 10%.

The invariant mass spectra were calculated for each pair of particles, $p\pi^0$, $p\eta$, and $\eta\pi^0$ of the final state. For this purpose only events having their beam energy lying within 5 narrow intervals of values ranging from 1.1 to 1.5 GeV were used and weighted by the inverse of the efficiency $\epsilon(E_\gamma, \theta_{\pi^0}, \theta_\eta)$. The stability in shape in terms of the efficiency was checked within the statistical errors using the efficiencies calculated with the various phase spaces generated in the simulation. The striking stability in shape originates from the large acceptance of the detector. The possible effect on the shape of the hole due to the missing events with $\theta_{\pi^0} \leq 12$ was also confirmed to be very small, when we compared the events generated in the simulation with and without cut on θ_{π^0}. In Fig. 3 we present the spectra with their areas normalized to give the total experimental cross section obtained at the same beam energy. The shape of the experimental spectra plotted with open circles is fully compatible with those generated with the phase space of $\gamma p \rightarrow \eta\Delta(1232)$ and plotted with dashed lines, reflecting the dominance of the $\eta\Delta$ production. The theoretical distributions plotted with thick continuous lines are normalized to give the central value of the total theoretical cross section obtained at the same beam energy. The uncertainty bands similar to the one on the total cross section are not shown here. The distributions show a narrow shape in the IM($p\eta$) spectra which is traced back to deficiencies in the model and comes from the width for

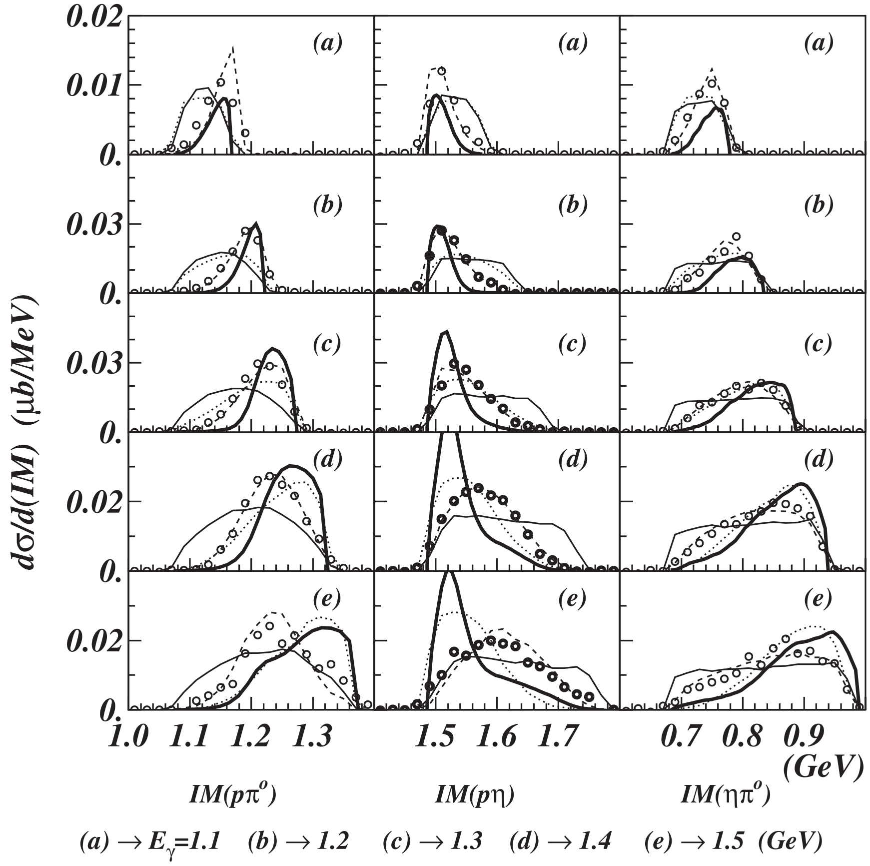

FIG. 3. For the reaction $\gamma p \to \eta\pi^0 p$, spectra of the invariant mass (IM) for ($p\pi^0$), ($p\eta$), and ($\eta\pi^0$) groups of the final state are presented in three different columns. The various rows, labeled (a), …, (e) correspond to beam energies given at the bottom of the columns. The open circles are the experimental results, the thin line is $\gamma p \to \eta\pi^0 p$ with a 3-body phase space in the final state, the dashed line is $\gamma p \to \eta\Delta$ with $\Delta \to \pi^0 p$, and the dotted line is $\gamma p \to \pi^0 S_{11}$ with $S_{11} \to \eta p$. The theoretical curves, given by thick lines, are the central values of the results of the model from Refs. [11,12].

the $N^*(1535)$ of about 90 MeV, consistent with the BES results [17], but does not account for the contribution of higher resonances such as the $N^*(1650)$. As shown in [11], the use of results of the empirical analysis for the $\pi N \to \eta N$ reaction [18] instead of the theoretical results leads to a somewhat wider distribution. As to the theoretical spectra in the IM($p\pi^0$) and IM($\eta\pi^0$) spectra, they agree better but one sees larger discrepancies at higher energies.

Similarly to the invariant mass spectra, the beam asymmetry observable Σ was also calculated for each pair of particles, $p\pi^0$, $p\eta$, and $\eta\pi^0$ of the final state and then plotted in Fig. 4. Doing so, three schemes of 2-body final state reactions were considered: (i) $\gamma p \to \eta X$ with $X \to p\pi^0$, (ii) $\gamma p \to \pi^0 Y$ with $Y \to \eta p$, and (iii) $\gamma p \to pZ$ with $Z \to \eta\pi^0$. This was done by using polarized photons in the horizontal plane and perpendicular to it. In each case the ϕ angle was the one from the sum of momenta of the pair considered with respect to a frame where the z direction is given by the photon momentum and the x, z plane is defined as the horizontal plane. Here, the experimental events were binned into 4 wide intervals of beam energy, 10 bins of invariant mass, and 12 bins of ϕ angle. The method of extracting Σ through the $\cos(2\phi)$ dependence was the same as in Ref. [14]. The experimental values in Fig. 4 are plotted with the errors originating from the fit of the $\cos(2\phi)$ dependence. The systematic error, not reported in the figure, is estimated to be 3% due to the beam polarization determination. Significant values are obtained with characteristic patterns. The comparison with the theoretical model results shows a good overall agreement. This agreement gives much valuable information on the dynamics of the process. Indeed, by looking at the IM(ηp) case, which has asymmetry values around -0.5, this can be traced in the model from [11,12] to the dominance of terms involving the coupling of $\Delta(1700)$ to $\eta\Delta$ and to $K\Sigma(1385)$. When these terms are removed this asymmetry becomes positive. The agreement with the asymmetries in the other cases is also spoiled by removing the $\Delta(1700)$ excitation term. This indicates that the $\Delta(1700)$ excitation mechanism is an essential ingredient to make sense of the different asymmetries measured in the experiment.

In summary, the novel experimental results and the comparison with the results of the model from Refs. [11,12] have shown that the observables reported in

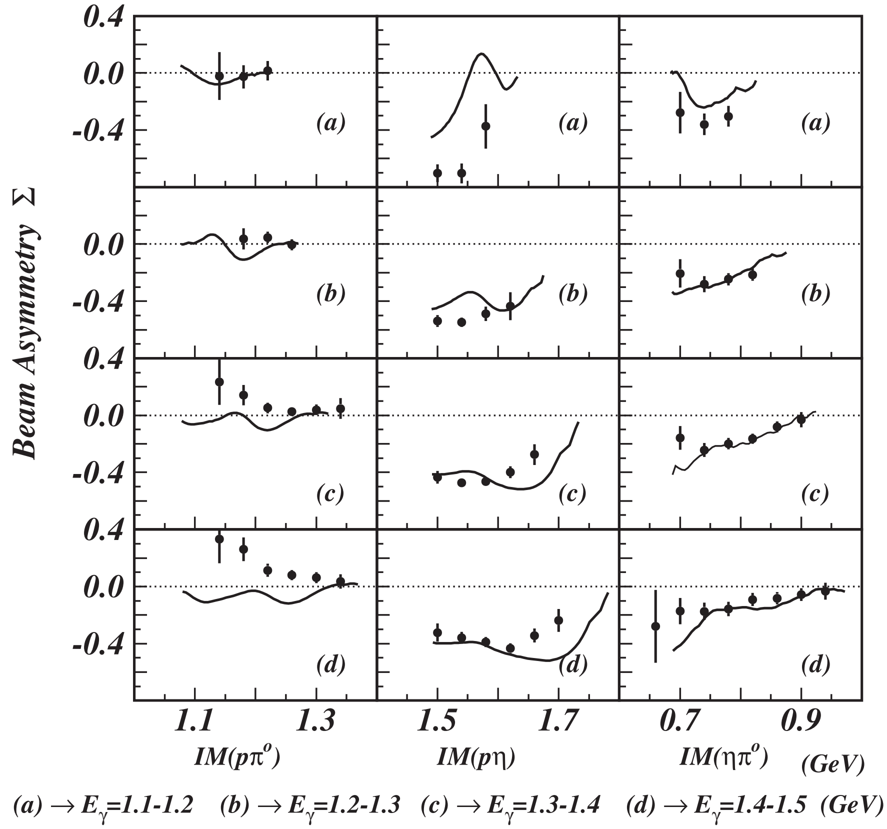

FIG. 4. Beam asymmetry of the reaction $\gamma p \rightarrow \eta \pi^0 p$. The theoretical results are calculated with the model of Refs. [11,12].

this Letter provide very valuable information concerning the basic reaction mechanisms and their strength. In particular, some important features of the reaction were traced back to the role played in the model by the $\Delta(1700)$ as being a dynamically generated resonance.

This work has been partially supported by DGCYT No. FIS2006-03438.

*hourany@ipno.in2p3.fr

[1] Y. Assafiri *et al.*, Phys. Rev. Lett. **90**, 222001 (2003).
[2] J. Ajaka *et al.*, Phys. Lett. B **651**, 108 (2007).
[3] V. Bernard, N. Kaiser, and U. G. Meissner, Int. J. Mod. Phys. E **4**, 193 (1995).
[4] G. Ecker, Prog. Part. Nucl. Phys. **35**, 1 (1995).
[5] N. Kaiser *et al.*, Phys. Lett. B **362**, 23 (1995).
[6] E. Oset and A. Ramos, Nucl. Phys. **A635**, 99 (1998).
[7] J. A. Oller and U. G. Meissner, Phys. Lett. B **500**, 263 (2001).
[8] T. Inoue, E. Oset, and M. J. Vicente Vacas, Phys. Rev. C **65**, 035204 (2002).
[9] E. E. Kolomeitsev and M. F. M. Lutz, Phys. Lett. B **585**, 243 (2004).
[10] S. Sarkar, E. Oset, and M. J. Vicente Vacas, Nucl. Phys. **A750**, 294 (2005); [**A780**, 90(E) (2006)].
[11] M. Döring, E. Oset, and D. Strottman, Phys. Rev. C **73**, 045209 (2006).
[12] M. Döring, E. Oset, and D. Strottman, Phys. Lett. B **639**, 59 (2006).
[13] D. Jido, M. Oka, and A. Hosaka, Prog. Theor. Phys. **106**, 873 (2001).
[14] J. Ajaka *et al.*, Phys. Rev. Lett. **81**, 1797 (1998).
[15] W. M. Yao *et al.* (PDG Collaboration), J. Phys. G **33**, 1 (2006).
[16] T. Nakabayashi *et al.*, Phys. Rev. C **74**, 035202 (2006).
[17] J. Z. Bai *et al.* (BES Collaboration), Phys. Lett. B **510**, 75 (2001).
[18] R. A. Arndt *et al.*, Phys. Rev. C **69**, 035213 (2004).